IJBBE International Journal of Biophotonics & Biomedical Engineering Vol. 5, No. 1, Spring-Summer, 2025

Review Article

Identifying Autism from EEG Signals Using Features Derived from Active Brain Source Models

M. Rajabioun*

**Mamaghan Branch, Islamic Azad University, Iran.*

***Corresponding Author Email: mrajabioun@iau.ac.ir**

DOI: 10.71498/ijbbe.2025.1204968

Received: Apr. 25, 2025, Revised: Jul. 21, 2025, Accepted: Jul. 22, 2025, Available Online: Sep. 4, 2025

ABSTRACT

Autism is a neurological condition that influences brain function and behavior, often becoming evident in early childhood and lasting into adulthood. It is characterized by challenges in social interaction, communication, and behavior, as well as decreased attention to the surrounding environment. Early identification and diagnosis of autism can play a crucial role in addressing its impacts and enhancing social and communication abilities. Various tools, like questionnaires and neurological techniques, are used for this purpose. One such technique is electroencephalography (EEG), which records the brain's electrical activity through sensors positioned on the scalp. This paper presents a method for identifying autism using EEG data. The process starts by pinpointing active brain sources through localization techniques, followed by the application of a dual Kalman filter to assess their activity. Features are subsequently derived from EEG signals using multivariate autoregressive moving average (MVARMA) and multivariate integrated autoregressive (ARIMA) models. Principal component analysis (PCA) is employed to identify essential features, and a K-nearest neighbor (KNN) classifier is utilized to classify individuals as either autistic or neurotypical. The proposed approach achieves higher accuracy and superior classification performance compared to existing methods, highlighting its effectiveness in identifying autism.

KEYWORDS

Dual Kalman Filter, Autoregressive moving average(ARMA) model, Autoregressive integrated moving average(ARIMA) model, Autism, Electroencephalography(EEG)

I. INTRODUCTION

Autism is an intricate neurodevelopmental condition with diverse manifestations and impacts. Individuals with autism often face challenges in expressing emotions, socializing, and adapting to new situations. Common signs include difficulty speaking, limited attention to surroundings, reduced emotional expression, and challenges in facially conveying feelings. These traits are particularly noticeable in children diagnosed with autism [1-3]. The condition typically emerges in early childhood or adolescence, with many adults on the autism spectrum also experiencing epilepsy or seizures at some point. This co-occurrence underscores the need for early diagnosis, comprehensive care, and tailored interventions for individuals with autism [4-7]. Evidence indicates a rising prevalence of autism diagnoses. A 2009 study by the Centers for Disease Control and Prevention (CDC) highlighted a consistent increase in cases. In the United States, autism prevalence rose from fewer than 3 per 10,000 children in the 1970s to over 30 per 10,000 by the 1990s. By 2012, the CDC revealed that autism was diagnosed in 1 out of every 88 children, including 1 in 54 boys. This increase highlights the critical need for early detection and intervention to enhance outcomes for individuals with autism [3, 7].

Various diagnostic methods aim to detect autism spectrum disorder (ASD) early, ensuring timely support and care. Each approach has strengths and limitations. Behavioral observation, for instance, involves closely monitoring a child's interactions, communication, and play. However, it is subject to observer bias and varying interpretations, leading to potential inconsistencies in diagnosis [8-10]. Standardized assessments such as the Autism Diagnostic Interview-Revised (ADI-R) and the Autism Diagnostic Observation Schedule (ADOS) have been developed to assess autism symptoms and severity[11, 12]. While these tools are valuable, reliance on self-reports or caregiver input can introduce biases and fail to capture the full range of behaviors. To overcome these challenges, researchers employ neuroimaging methods, such as functional magnetic resonance imaging (fMRI) and electroenc ephalography (EEG), to study brain function and connectivity in those with autism. These methods offer insights into the neural underpinnings of autism and may help identify biomarkers for diagnosis [12-15]. EEG, in particular, is a non-invasive and cost-effective method that captures the brain's electrical function through scalp electrodes. It is especially useful for studying brain rhythms and connectivity patterns associated with autism[15, 16]. EEG's ability to capture rapid changes in brain activity makes it an invaluable tool for identifying and understanding autism. By leveraging EEG data, researchers can facilitate early diagnosis, develop tailored interventions, and improve treatment outcomes.

Identifying autism through EEG signals has become a key area of interest in neuroscience, with numerous studies investigating novel approaches. Many of these studies have applied machine learning algorithms to EEG data, resulting in impressive accuracy in differentiating individuals with autism from those without the condition. [17-23]. Advanced deep learning techniques have also been suggested to extract crucial features from EEG signals, demonstrating encouraging outcomes in the identification of autism [24-27]. For example, Schwartz et al. examined specific frequency bands of EEG, identifying unique patterns associated with autism [28, 29]. Innovative methods that merge EEG analysis with graph theory, pioneered by Jurriaan and Precenzano et al., offer new insights into autism detection [30]. Tawhid et al. applied time-frequency analysis to reveal the dynamic patterns of the EEG associated with autism[31]. Additionally, Landowska integrated EEG with physiological data, such as heart rate and skin conductance, enhancing diagnostic accuracy[32]. Qaysar explored advanced signal processing methods such as wavelet transforms and independent component analysis, uncovering distinctive EEG patterns associated with autism [33]. Collectively, these methods highlight global efforts to enhance autism detection through EEG analysis, contributing to the development of more accurate diagnostic tools.

Research has also highlighted unusual patterns of connectivity in the brains of people with autism. Studies indicate heightened local connectivity and diminished long-range connections in individuals with autism[34-39]. Wass et al. discovered enhanced connectivity in frontal and short-range neural pathways, whereas Coben et al. noted increased frontal coherence and reduced coherence in posterior temporal regions[36]. Granger causality analyses revealed weakened connectivity between distant brain areas, particularly in the prefrontal cortex, anterior cingulate, and inferior parietal regions[37]. Coben et al.

further confirmed this reduced connectivity during tasks involving emotional processing[40], Similarly, Minshew and Williams reported increased frontal coherence but diminished connectivity between anterior and posterior temporal regions in autism[41]. Using dynamic causal modeling on fMRI data, Wataru Sato et al. identified decreased activity in the visual regions of the brain in children with autism [42].

This study introduces an innovative method that applies multivariate autoregressive moving average (MVARMA) and multivariate autoregressive integrated moving average (MVARIMA) models to detect autism. Key features are derived from the model parameters, highlighting the statistical properties of important ARMA and ARIMA parameters. The methodology begins with source localization to isolate active brain regions from EEG signals, then utilizes a dual Kalman filter to estimate the activities and interactions of these sources. EEG signals are mapped from sensor space to source space, where MVARMA and MVARIMA models are used to analyze these time series, incorporating past signal and source activity data. Assessing source dynamics, which represent temporal variations in brain activity, is a crucial and challenging step. Traditional methods like dynamic causal modeling (DCM) use linear or nonlinear frameworks for neural connections calculation, assuming nonlinear relationships between neural dynamics[43-45]. Moreover, dual Kalman filter methods are commonly employed to estimate dynamic source activity[46, 47]. Dual Kalman filter techniques are also employed for this purpose. For example, A.H. Omidvarnia employed dual Kalman filters on newborn EEG data[48], while Eduardo Giraldo introduced a comparable method for estimating source activity. Rajabioun et al. utilized a dual Kalman filter technique to investigate effective connectivity in EEG data from individuals with autism, revealing distinct differences between autistic and neurotypical subjects [47]. These advanced techniques demonstrate significant progress in analyzing brain dynamics and improving autism diagnosis through EEG.

II. MATERIALS AND METHODS

This study proposes a technique for distinguishing individuals with autism from neurotypical participants. This classification is crucial for halting the disorder's progression and enhancing the quality of life for affected individuals. The detailed diagram of the method is illustrated in Figure 1.

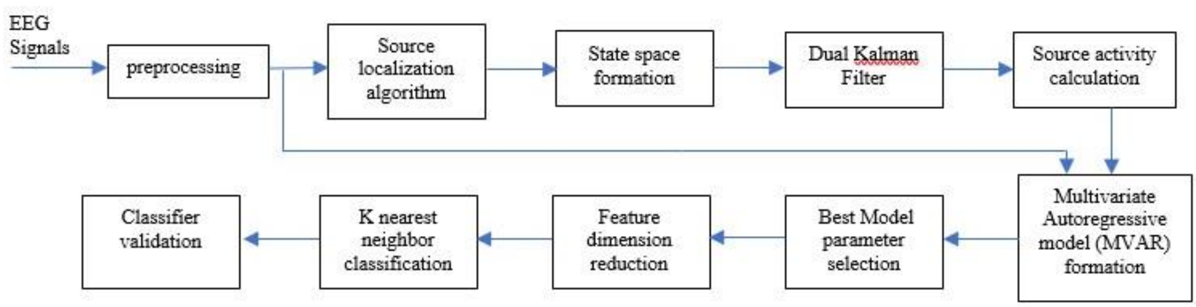

Fig. **1** The proposed method's flowchart is structured around features derived from MVAR parameters, with source activity as the input and EEG signals as the output time series.

The first step involves acquiring or preparing EEG signals. The signal that are used in this paper was sourced from a publicly available dataset [49]. The dataset comprises EEG recordings obtained with the Biosemi ActiveTwo system from 28 participants diagnosed with autism spectrum conditions and 28 neurotypical individuals, ranging in age from 18 to 68 years. The data was collected during a 150-second resting state with eyes closed. Ethical approval for the study, including data collection and sharing, was provided by the Health Research Authority under IRAS ID 212171[49].

After preprocessing, the filtered EEG signals undergo a source localization procedure to identify and estimate the active brain regions or sources. This step simplifies the complexity of the data by selecting a finite set of active sources and mapping their spatial coordinates. The objective of source localization is to minimize a specific function, ultimately pinpointing active brain regions.

Raw EEG signals are preprocessed to remove noise and artifacts. This process begins with a bandpass Butterworth filter applied to restrict frequencies to the range of 0.5–100 Hz, reducing unwanted noise. Independent component analysis (ICA) is then performed to isolate components linked to brain activity. Non-brain-related components, such as those associated with eye blinks, electromyography (EMG), 50 Hz powerline interference, and auditory artifacts, are identified and removed, leaving a clean signal. For detailed methodologies on artifact removal and brain-component identification, refer to [50-52].

$$F = \|V_K - GJ_K\| + \alpha\|J_K\| \qquad (1)$$

where $V_K(m \times 1)$ is the recorded signal recorded at the Kth sample, $J_K(3n \times 1)$ denotes the brain's source activity for the Kth sample and G$(m \times 3n)$ is the leadfield matrix, which is computed through forward problem-solving methods[53, 54]. This function is divided into two primary components: one accounts for error estimation, while the other manages noise reduction and smooths abrupt changes in source activities. The balance between these components is controlled by a parameter, α, which is determined using algorithms such as Tikhonov regularization or the L-curve method [55].

Several strategies are available to minimize Equation 1, with one widely used method being sLORETA. This approach is particularly effective due to its ability to achieve zero localization error [55, 56]. In sLORETA, the explicit solution can be obtained using the given values of G and V_K:

$$\widehat{J_K} = T.V_K \qquad (2)$$

The approximated brain source activity, denoted as $\widehat{J_K}(3n \times 1)$, can be derived using the transformation matrix T$(3n \times m)$, which links the recorded EEG signals (V_K) to the estimated source activities. In sLORETA, TT is calculated as follows:

$$T = G^T H[HGG^T H + \alpha H]^+ \qquad (3)$$

where $[\quad]^+$ denotes the pseudoinverse of the matrix, and HH is the regularization matrix used to ensure smoothness. HH is defined as:

$$H = I - 11^T/1^T 1 \qquad (4)$$

In this equation, I denotes a unit matrix, and 1 refers to a column vector of ones with dimensions (m×1). These components are essential for selecting active regions. The source activity estimation method (Eq. 2) is applied to time-varying EEG signals to detect active brain regions. For each sample, the estimation identifies specific sources as active. Regions with the highest probability of activity across samples are selected, representing areas of significant neural engagement.

Once the active sources are identified, a model of linear variations is applied to capture their temporal dynamics. The model is expressed as:

$$J_K = F_K J_{K-1} + \eta_K \qquad (5)$$

where η_K represents state noise, and F_K is the relationship matrix at the Kth sample, characterizing dependencies between active regions and their self-relation over time. The connection between these sources and the EEG signals is established through the leadfield matrix, which is calculated using forward modeling techniques. This relationship can be summarized as follows:

$$\begin{cases} J_K = F_K J_{K-1} + \eta_K \\ V_K = G J_K + \varepsilon_K \end{cases} \tag{6}$$

Where η_K represents measurement noise. Both J_K (a source activity over time) and

F_K (spatiotemporal relationship matrix) are estimated using a dual Kalman filter, as detailed in [57, 58]. After source activity (J_K) changes calculation, a multivariate autoregressive moving average (ARMA) model is fitted to recorded signals. This model relates V_K to its past values and the estimated source activity

J, expressed as:

$$V_K = \sum_{i=1}^{p} a_i V_{K-i} + \sum_{i=0}^{q} b_i J_{K-i} \tag{7}$$

where a_i, b_i are parameter matrices, with a_i (m×p), and b_i (n×(q+1)), corresponding to the dimensions of V (m) and J (n).

To address the nonstationary nature of EEG signals, an autoregressive integrated moving average (ARIMA) model is also utilized. The ARIMA(p,d,q) model is defined as:

$$V_K = \sum_{i=1}^{p} a_i V_{K-i} + \sum_{i=0}^{q} b_i J_{K-i} + \sum_{i=1}^{d} c_i (1-Z)^d Y_i \tag{8}$$

Here, Z is the delay operator, and the difference operator is defined as:

$$\begin{aligned} (1-Z)Y_i &= Y_i - Y_{i-1} \\ (1-Z)^2 Y_i &= Y_i - 2Y_{i-1} + Y_{i-2} \\ &\dots \end{aligned} \tag{9}$$

These models provide a robust framework for analyzing EEG data by leveraging both stationary and nonstationary signal characteristics, enabling more accurate assessments of brain dynamics.

In this part of the discussion, the activities from the sources act as the model's input, whereas the resultant EEG signals represent the output. The objective is to model each EEG sample by utilizing its delayed versions and the associated source activities. To accomplish this, matrices associated with the ARMA and ARIMA models—referred to as ‘a’, ‘b’, and ‘c’—are calculated for every sample. The dimensions of these matrices are determined by the respective orders of the models.

Next, various characteristics are derived from these model parameters to assist with classification. To simplify the process, the parameters are divided into two distinct classes, with features extracted from each:

- **Class 1:** Parameters with low variability, indicated by a standard deviation of less than 20% of the average value. The mean values of these parameters are utilized to form the feature vectors.

- **Class 2:** Parameters that display a higher degree of variability compared to those in Class 1. For this class, the following statistical metrics are selected for the feature vector:

- Average signal value
- Standard deviation of the signal
- Signal kurtosis
- Signal skewness
- Signal entropy

Subsequently, horizontal and natural visibility graphs are created from each time series array, and several features are then extracted from them. Further details on visibility graphs can be found in [60, 62, 63]. Key features include:

- Average value of the graph nodes

• Standard deviation of the graph nodes

• Mean length of the shortest path from each node to all other nodes

After constructing the feature vectors, dimensionality reduction techniques are employed to reduce complexity and enhance classification accuracy. PCA, or principle component analysis, is employed as an effective method for reducing the dimensionality of the feature vectors. PCA converts a collection of potentially interrelated, high-dimensional features into a new set of independent variables, referred to as principal components. This process preserves the most important information from the original features while minimizing their dimensionality. PCA begins with the normalization of each feature, centering it by subtracting its mean. Next, a correlation matrix is created from these normalized features, followed by the computation of eigenvalues. The eigenvectors associated with the largest eigenvalues are then chosen to form a transformation matrix. This matrix transforms the original feature vector into a lower-dimensional space, effectively reducing its dimensions while retaining essential information.

Finally, a Support Vector Machine (SVM) is employed to classify and distinguish depressive subjects from normal individuals. SVM is chosen for its excellent performance in classifying high-dimensional feature spaces. It works by finding a hyperplane that maximizes the margin between classes, focusing on the nearest data points known as support vectors. While this is a brief overview, more detailed information on SVM mechanisms and optimization techniques can be found in the relevant literature. SVM is a widely used classifier, renowned for its robustness in managing complex classification tasks.

III. SIMULATION AND RESULTS

This part describes the application of the suggested approach to EEG data obtained from both individuals with autism and neurotypical participants. The procedure involved multiple stages, starting with the retrieval and recording of EEG signals from a reliable source. Next, the signals underwent preprocessing, which included the application of a bandpass filter designed to retain frequencies within the range of 0.5 to 30 Hz. Following this, ICA is applied to the signals to extract independent components, aiming to remove those unrelated to brain function, like blinking, EMG or ECG interference, 50Hz noise, and auditory brain responses. Detailed descriptions of the methods used to identify and remove these artifacts can be found in [50-52]. After preprocessing, the signals were processed using sLORETA(standardized low-resolution electromagnetic tomography) to extract the underlying brain sources with zero localization error [55, 56]. The regularization parameter for sLORETA was established through the use of the Tikhonov regularization technique [54]. Afterward, active sources were identified during the EEG recording process, and the most significant ones were selected based on their overall performance throughout the dataset. The number of EEG channels determined the selection of sources, after which a multivariate autoregressive (MVAR) model was applied to examine the identified active sources. This process led to the development of a state-space model that captures the interactions between the EEG channels and these sources. A dual Kalman filter was employed to simultaneously estimate dynamic source activity and compute the relationship matrix. Additionally, an autoregressive moving average (ARMA) or autoregressive integrated moving average (ARIMA) model was utilized to establish a connection between the source activity as input and the EEG channel recordings as output. Following this, statistical and graph-based features were extracted from the parameters estimated by the ARMA or ARIMA model. Principal Component Analysis (PCA) was then applied to reduce the dimensionality of these features, compressing the feature vector to 15 components. In the final step, a Support Vector Machine (SVM) was trained using the reduced feature set, allowing for classification based on the SVM model. To assess the classification performance, multiple simulations were carried out to examine the impact of different parameter variations. Additionally, various performance metrics were defined to validate the classification outcomes.

$$Accurency = \frac{TP+TN}{TP+TN+FP+FN}$$
(Eq. 10)

$$sensitivity = \frac{TP}{TP+FN}$$
(Eq. 11)

$$specificity = \frac{TN}{TN+FP} \quad (12)$$

Firstly, the classification was conducted by altering the ARMA model's order. Different orders of models were tested for both the ARMA and ARIMA models (as described in Equation 7), and the results for each configuration are presented in Table 1.

Table 1. The proposed method evaluated the accuracy, sensitivity, and specificity of EEG classification between autistic and control groups, utilizing different orders of the ARMA and ARIMA models.

	ARMA(2,2)	ARMA(4,2)	ARMA(4,3)	ARMA(5,4)	ARMA(6,5)
Accuracy	0.9107	0.9286	0.9464	0.9821	0.9464
Sensitivity	0.9286	0.9643	0.9643	1	0.9643
Specificity	0.8929	0.8929	0.9286	0.9643	0.9286
	ARIMA(2,1,2)	ARIMA(4,2,2)	ARIMA(4,2,3)	ARIMA(4,3,4)	ARIMA(6,4,5)
Accuracy	0.9286	0.9821	0.9821	1	0.9464
Sensitivity	0.9643	0.9643	1	1	0.9643
Specificity	0.9286	0.9286	0.9643	1	0.9286

The data presented in Table 1 show that the ARMA(5,4) model exceeds the performance of all other models. Previous research has suggested several methods for determining model order, one of which is the Akaike Information Criterion (AIC) approach[59, 60]. By applying this method, the optimal ARMA model order was identified as ARMA(5,5), which closely resembles the ARMA(5,4) model that demonstrated superior performance in this study. For the ARIMA model, both ARIMA(4,2,3) and ARIMA(4,3,4) provided superior results compared to the other configurations. This indicates that the ARIMA model delivers more accurate results than the ARMA model when using the same order, highlighting its advantage in handling nonstationary signals due to the inclusion of differencing operations.

In the second simulation, the effect of two feature types is analyzed. First, classification is performed using only statistical features, followed by classification using features extracted from visibility graphs. Next, classification is performed by combining both statistical and visibility graph features. Figure 2 displays the classification accuracies for the models ARMA(4,3), ARMA(5,4), ARIMA(4,2,3), and ARIMA(4,3,4).

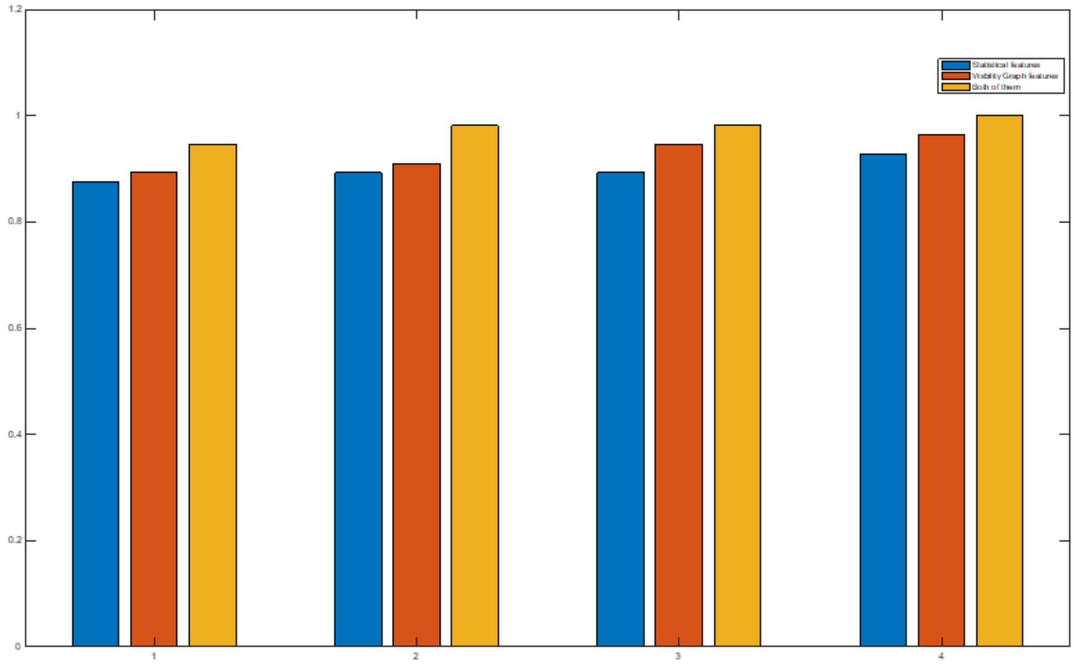

Fig. **2** The classification accuracy using the proposed method is evaluated based on different feature sets (statistical, visibility graph, and a combination of both). The classification is performed using various models, including ARMA(4,3), ARMA(5,4), ARIMA(4,2,3), and ARIMA(4,3,4).

In the second simulation, classifiers that were trained with features derived from visibility graphs showed higher accuracy compared to those trained solely with statistical features. This enhancement can be credited to the additional structural information captured by visibility graphs. As seen in Figure 2, the ARIMA(4,3,4) model outperforms other models, such as ARMA(4,3), ARMA(5,4), and ARIMA(4,2,3), highlighting its ability to better capture the inherent patterns and dynamics within the data, resulting in improved classification accuracy.

In the third simulation, the impact of decreasing the feature count through PCA is explored. While the previous simulations reduced the feature set to 15, this simulation evaluates various feature set sizes (5, 10, 15, 20, 30, and 50) and examines the corresponding classification accuracy and simulation time. Table 2 presents the results of this simulation, which was conducted using the ARMA(5,4) and ARIMA(4,3,4) models.

Table **2**. The results show the accuracy and simulation time of the proposed method with different numbers of features reduced by PCA, using the ARMA(5,4) and ARIMA(4,3,4) models.

	5	10	15	20	30	50
Accuracy (ARMA(5,4))	0.8929	0.9464	0.9821	0.9821	1	1
Simulation time (ARMA(5,4)) In sec	762	983	1463	2873	3182	8982
Accuracy (ARMA(5,4))	0.9286	0.9821	1	1	1	1
Simulation time (ARIMA(4,3,4)) In sec	1282	1676	3593	4282	7083	10012

The findings in Table 2 indicate that a larger feature set for SVM training enhances accuracy but also extends the simulation time, highlighting an increased computational burden. Notably, after selecting 15 features, further increases in the number of features do not yield significant improvements in accuracy, though the computational cost keeps increasing. Thus, it is recommended to strategically determine the reduced feature count through PCA, with 15 features providing an optimal balance between computational efficiency and accuracy.

Lastly, the performance of the proposed method was compared to other methods used for recognizing autistic individuals. The proposed method, along with approaches from previous studies, was tested on the same dataset, and their classification accuracies are shown in Table 3.

Table **3**. Comparison of Classification Accuracy for Autism Recognition Using Various Methods from Previous Studies

	Method No.1(48)	Method No.2 (20)	Method No.3(24)	Method No.4 (32)	Proposed method ARMA(5,4)	Proposed method ARIMA(4,3,4)
Accuracy	0.8929	0.9464	0.9464	0.9643	0.9821	1

The results from Table 3 show that the method which are proposed by this paper outperforms other methods in terms of classification accuracy. Specifically, using ARIMA(4,3,4) improves the classification performance. However, it is essential to recognize that this method demands more computational time than the ARMA(5,4) approach. ARMA models are typically favored when minimizing simulation time is a priority.

IV. DISCUSSION

This research introduces an innovative approach to identifying individuals with autism by utilizing EEG signals and features extracted from multivariate autoregressive moving average (MVARMA) and multivariate integrated autoregressive (ARIMA) models. The approach consists of multiple essential steps, including source localization, source activity estimation using a dual Kalman filter, and parameter computation through MVARMA and ARIMA models. PCA is employed to identify key parameters, followed by classification using a K-nearest neighbor (KNN) classifier. The findings highlight improved classification accuracy over other methods, underscoring the effectiveness of this approach. The main objective is to use EEG signals to differentiate autistic participants from neurotypical individuals by estimating source activities and capturing the altered dynamics and connectivity between brain sources linked to autism.

To evaluate the effectiveness of the method, a series of simulations was performed to examine the effects of various parameter adjustments. The results presented in Table 1 demonstrate that the ARMA(5,4) and ARIMA(4,3,4) models performed better than other configurations, with the Akaike method suggesting that the ARMA(5,5) model is comparable to the superior ARMA(5,4) model. In the case of the ARIMA model, both ARIMA(4,2,3) and ARIMA(4,3,4) showed improved performance, emphasizing the benefit of ARIMA in handling nonstationary signals through its differencing process.

Additional simulations examined the effect of various features on classification accuracy, revealing that features derived from high visibility graphs (HVG) and non-visible graphs (NVG) play a crucial role in enhancing the results. Combining these graph-based features with statistical features led to better performance. As numerous features increased computational load, PCA was used for feature dimensionality reduction. The findings suggested that reducing features improves accuracy but increases computation time, necessitating an optimal trade-off between computational efficiency and accuracy.

Finally, the method's performance was compared with other approaches, demonstrating that ARIMA(4,3,4) offers superior results. In conclusion, this research introduces a robust approach for identifying autism using EEG signals and features extracted from MVARMA/ARIMA models. The approach shows promise for gaining deeper insights into brain dynamics and connectivity associated with autism, through analysis of parameter variations and feature selection.

V. Conclusion

This study addresses autism spectrum disorder, a multifaceted condition impacting people across their lifespan, characterized by unique patterns of interaction, behavior, and communication, coupled with limited attention to external stimuli. Early detection is essential for intervention and enhancing interpersonal and communicative abilities. There are several techniques available for identifying autism, with one being EEG (electroencephalogram), which monitors electrical brain activity through sensors placed on the scalp. EEG signals offer valuable insights into brain activity, helping to explore the neurological processes associated with autism. Our approach estimates the activity of brain sources and analyzes the connectivity between regions to uncover patterns and dynamics unique to autism.

We present a method that leverages EEG signals and features extracted from MVARMA (Multivariate Autoregressive Moving Average) and ARIMA (Autoregressive Integrated Moving Average) models for autism classification. These models effectively capture dependencies in the data, statistical traits, and the nonstationarity often observed in brain activity associated with autism. Our method outperforms existing alternatives by accurately distinguishing autistic individuals from neurotypical participants. The method involves several essential stages: preprocessing the signals, localizing sources, modeling, extracting features, and performing classification. Through simulations and adjustments to parameters, we determine the ideal model configurations and features that optimize classification performance.

The study emphasizes the significance of comprehending brain source dynamics and connectivity in relation to autism. By analyzing recorded signals and applying MVARMA and ARIMA models, the study uncovers brain activity patterns in individuals with autism. PCA is used for feature reduction, which enhances computational efficiency while preserving accuracy. Selecting between ARIMA and ARMA models requires a trade-off between accuracy and simulation duration, with ARMA models being better suited for quicker simulations.

In summary, this research introduces a powerful approach for accurate autism identification through EEG data, which can support early diagnosis and therapeutic measures. Future studies involving larger and more varied datasets will strengthen the method's reliability and broaden its applicability. Investigating the method's applicability to various demographic groups and age ranges is crucial. Advances in EEG technology offer the potential to enhance autism detection, paving the way for tailored interventions and improved outcomes for those affected by the condition.

Reference

[1] A. Jack and J. P. Morris, "Neocerebellar contributions to social perception in adolescents with autism spectrum disorder," (in eng), Dev Cogn Neurosci, vol. 10, pp. 77-92, 2014.

[2] J. Grèzes, B. Wicker, S. Berthoz, and B. de Gelder, "A failure to grasp the affective meaning of actions in autism spectrum disorder subjects," Neuropsychologia, vol. 47, no. 8, pp. 1816-1825, 2009.

[3] W. Sato, M. Toichi, S. Uono, and T. Kochiyama, "Impaired social brain network for processing dynamic facial expressions in autism spectrum disorders," (in eng), BMC Neurosci, vol. 13, p. 99, 2012.

[4] P. Shih, M. Shen, B. Ottl, B. Keehn, M. S. Gaffrey, and R. A. Müller, "Atypical network connectivity for imitation in autism spectrum disorder," (in eng), Neuropsychologia, vol. 48, no. 10, pp. 2931-2939, 2010.

[5] I. Mohammad-Rezazadeh, J. Frohlich, S. K. Loo, and S. S. Jeste, "Brain connectivity in autism spectrum disorder," (in eng), Curr Opin Neurol, vol. 29, no. 2, pp. 137-47, 2016.

[6] X. Yang, N. Zhang, and P. Schrader, "A study of brain networks for autism spectrum disorder classification using resting-state functional connectivity," Machine Learning with Applications, vol. 8, pp. 100290, 2022.

[7] M. K. Belmonte, G. Allen, A. Beckel-Mitchener, L. M. Boulanger, R. A. Carper, and S. J. Webb, "Autism and abnormal development of brain connectivity," (in eng), J Neurosci, vol. 24, no. 42, pp. 9228-9231, 2004.

[8] N. Bauminger-Zviely and A. Shefer, "Naturalistic evaluation of preschoolers' spontaneous interactions: The Autism Peer Interaction Observation Scale," (in eng), Autism, vol. 25, no. 6, pp. 1520-1535, 2021.

[9] J. Richer, "The social-avoidance behaviour of autistic children," Animal Behaviour, vol. 24, no. 4, pp. 898-906, 1976.

[10] P. Wei, D. Ahmedt-Aristizabal, H. Gammulle, S. Denman, and M. A. Armin, "Vision-based activity recognition in children with autism-related behaviors," Heliyon, vol. 9, no. 6, pp. e16763, 2023.

[11] T. Sappok et al., "Diagnosing autism in a clinical sample of adults with intellectual disabilities: How useful are the ADOS and the ADI-R?," Research in Developmental Disabilities, vol. 34, no. 5, pp. 1642-1655, 2013.

[12] C. Lord and R. Luyster, "Early diagnosis of children with autism spectrum disorders," Clinical Neuroscience Research, vol. 6, no. 3, pp. 189-194, 2006.

[13] M. Baygin et al., "Automated ASD detection using hybrid deep lightweight features extracted from EEG signals," Computers in Biology and Medicine, vol. 134, pp. 104548, 2021.

[14] S. N. Seyed Fakhari, F. Ghaderi, M. Tehrani-Doost, and N. Moghadam Charkari, "EEG-based brain connectivity analysis in autism spectrum disorder: Unraveling the effects of bumetanide treatment," Biomedical Signal Processing and Control, vol. 86, pp. 105054, 2023.

[15] E. L. Juarez-Martinez et al. "Prediction of Behavioral Improvement Through Resting-State Electroencephalography and Clinical Severity in a Randomized Controlled Trial Testing Bumetanide in Autism Spectrum Disorder," Biological Psychiatry: Cognitive Neuroscience and Neuroimaging, vol. 8, no. 3, pp. 251-261, 2023.

[16] W. J. Bosl, H. Tager-Flusberg, and C. A. Nelson, "EEG Analytics for Early Detection of Autism Spectrum Disorder: A data-driven approach," Scientific Reports, vol. 8, no. 1, pp. 6828, 2018.

[17] S. Peketi and S. B. Dhok, "Machine Learning Enabled P300 Classifier for Autism Spectrum Disorder Using Adaptive Signal Decomposition," (in eng), Brain Sci, vol. 13, no. 2, 2023.

[18] S. Raj and S. Masood, "Analysis and Detection of Autism Spectrum Disorder Using Machine Learning Techniques," Procedia Computer Science, vol. 167, pp. 994-1004, 2020.

[19] D. D. Khudhur and S. D. Khudhur, "The classification of autism spectrum disorder by machine learning methods on multiple datasets for four age groups," Measurement: Sensors, vol. 27, pp. 100774, 2023.

[20] B. Ari, N. Sobahi, Ö. F. Alçin, A. Sengur, and U. R. Acharya, "Accurate detection of autism using Douglas-Peucker algorithm, sparse coding based feature mapping and convolutional neural network techniques with EEG signals," Computers in Biology and Medicine, vol. 143, pp. 105311, 2022.

[21] A. R. Aslam and M. A. B. Altaf, "Chapter 14 - Machine learning–based patient-specific processor for the early intervention in autistic children through emotion detection," in Neural Engineering Techniques for Autism Spectrum Disorder, A. S. El-Baz and J. S. Suri Eds.: Academic Press, 2021, pp. 287-313.

[22] S. Parui, D. Samanta, N. Chakravorty, U. Ghosh, and J. J. P. C. Rodrigues, "Artificial intelligence and sensor-based autism spectrum disorder diagnosis using brain connectivity analysis," Computers and Electrical Engineering, vol. 108, pp. 108720, 2023.

[23] J. Strzelecka, "Electroencephalographic studies in children with autism spectrum disorders," Research in Autism Spectrum Disorders, vol. 8, no. 3, pp. 317-323, 2014.

[24] A. S. Mohanty, P. Parida, and K. C. Patra, "ASD classification for children using deep neural network," Global Transitions Proceedings, vol. 2, no. 2, pp. 461-466, 2021.

[25] L. Xu et al., "Characterizing autism spectrum disorder by deep learning spontaneous brain activity from functional near-infrared spectroscopy," Journal of Neuroscience Methods, vol. 331, pp. 108538, 2020.

[26] C. Li, T. Zhang, and J. Li, "Identifying autism spectrum disorder in resting-state fNIRS signals based on multiscale entropy and a two-branch deep learning network," Journal of Neuroscience Methods, vol. 383, pp. 109732, 2023.

[27] T. M. Epalle, Y. Song, Z. Liu, and H. Lu, "Multi-atlas classification of autism spectrum disorder with hinge loss trained deep architectures: ABIDE I results," Applied Soft Computing, vol. 107, pp. 107375, 2021.

[28] S. Schwartz, R. Kessler, T. Gaughan, and A. W. Buckley, "Electroencephalogram Coherence Patterns in Autism: An Updated Review," (in eng), Pediatr Neurol, vol. 67, pp. 7-22, 2017.

[29] F. Precenzano et al. "Electroencephalographic Abnormalities in Autism Spectrum Disorder: Characteristics and Therapeutic Implications," (in eng), Medicina (Kaunas), vol. 56, no. 9, 19 2020.

[30] J. M. Peters et al., "Brain functional networks in syndromic and non-syndromic autism: a graph theoretical study of EEG connectivity," BMC Medicine, vol. 11, no. 1, pp. 54, 2013.

[31] M. N. A. Tawhid, S. Siuly, and H. Wang, "Diagnosis of autism spectrum disorder from EEG using a time–frequency spectrogram image-based approach," Electronics Letters, vol. 56, no. 25, pp. 1372-1375, 2020.

[32] A. Landowska et al., "Automatic Emotion Recognition in Children with Autism: A Systematic Literature Review," Sensors, vol. 22, no. 4, pp. 1649, 2022.

[33] Q. Mohi-Ud-Din and A. K. Jayanthy, "WITHDRAWN: EEG feature extraction using wavelet transform for classifying autism spectrum disorder," Materials Today: Proceedings, 2021.

[34] L. Cornew, T. P. Roberts, L. Blaskey, and J. C. Edgar, "Resting-state oscillatory activity in autism spectrum disorders," (in eng), J Autism Dev Disord, vol. 42, no. 9, pp. 1884-1894, 2012.

[35] J. R. Isler, K. M. Martien, P. G. Grieve, R. I. Stark, and M. R. Herbert, "Reduced functional connectivity in visual evoked potentials in children with autism spectrum disorder," (in eng), Clin Neurophysiol, vol. 121, no. 12, pp. 2035-2043, 2010.

[36] S. Wass, "Distortions and disconnections: disrupted brain connectivity in autism," (in eng), Brain Cogn, vol. 75, no. 1, pp. 18-28, 2011.

[37] M. E. Vissers, M. X. Cohen, and H. M. Geurts, "Brain connectivity and high functioning autism: a promising path of research that needs refined models, methodological convergence, and stronger behavioral links," (in eng), Neurosci Biobehav Rev, vol. 36, no. 1, pp. 604-25, 2012.

[38] P. Barttfeld et al. "State-dependent changes of connectivity patterns and functional brain network topology in autism spectrum disorder," (in eng), Neuropsychologia, vol. 50, no. 14, pp. 3653-3662, 2012.

[39] L. Q. Uddin, K. Supekar, and V. Menon, "Reconceptualizing functional brain connectivity in autism from a developmental perspective," (in eng), Front Hum Neurosci, vol. 7, pp. 458, 2013.

[40] R. Coben, I. Mohammad-Rezazadeh, and R. L. Cannon, "Using quantitative and analytic EEG methods in the understanding of connectivity in autism spectrum disorders: a theory of mixed over- and under-connectivity," (in eng), Front Hum Neurosci, vol. 8, pp. 45, 2014.

[41] N. J. Minshew and D. L. Williams, "The new neurobiology of autism: cortex, connectivity, and neuronal organization," (in eng), Arch Neurol, vol. 64, no. 7, pp. 945-50, 2007.

[42] W. Sato, M. Toichi, S. Uono, and T. Kochiyama, "Impaired social brain network for processing dynamic facial expressions in autism spectrum disorders," BMC Neuroscience, vol. 13, no. 1, pp. 99, 2012.

[43] E. A. Aponte, S. Raman, B. Sengupta, W. D. Penny, K. E. Stephan, and J. Heinzle, "mpdcm: A toolbox for massively parallel dynamic causal modeling," (in eng), J Neurosci Methods, vol. 257, pp. 7-16, 15 2016.

[44] J. Nováková, M. Hromčík, and R. Jech, "Dynamic Causal Modeling and subspace identification methods," Biomedical Signal Processing and Control, vol. 7, no. 4, pp. 365-370, 2012.https://doi.org/10.1016/j.bspc.2011.07.002.

[45] M. Pyka, D. Heider, S. Hauke, T. Kircher, and A. Jansen, "Dynamic causal modeling with genetic algorithms," Journal of Neuroscience Methods, vol. 194, no. 2, pp. 402-406, 2011.

[46] M. Rajabioun, A. M. Nasrabadi, and M. B. Shamsollahi, "Estimation of effective brain connectivity with dual Kalman filter and EEG source localization methods," (in eng), Australas Phys Eng Sci Med, vol. 40, no. 3, pp. 675-686, 2017.

[47] M. Rajabioun, A. Motie Nasrabadi, M. B. Shamsollahi, and R. Coben, "Effective brain connectivity estimation between active brain regions in autism using the dual Kalman-based method," (in eng), Biomed Tech (Berl), vol. 65, no. 1, pp. 23-32, 28 2020.

[48] A. H. Omidvarnia, M. Mesbah, M. S. Khlif, J. M. O'Toole, P. B. Colditz, and B. Boashash, "Kalman filter-based time-varying cortical connectivity analysis of newborn EEG," (in eng), Annu Int Conf IEEE Eng Med Biol Soc, vol. 2011, pp. 1423-1426, 2011.

[49] E. Milne, *EEG Data for Electrophysiological signatures of brain aging in autism spectrum disorder* ed, The University of Sheffield, 2021.

[50] S. Makeig and J. Onton, *ERP features and EEG dynamics: An ICA perspective*, The Oxford Handbook of Event-Related Potential Components, 2012.

[51] J. Onton and S. Makeig, "Information-based modeling of event-related brain dynamics," (in eng), Prog Brain Res, vol. 159, pp. 99-120, 2006.

[52] A. Delorme and S. Makeig, "EEGLAB: an open source toolbox for analysis of single-trial EEG dynamics including independent component analysis," (in eng), J Neurosci Methods, vol. 134, no. 1, pp. 9-21, 2004.

[53] K. A. Awada, D. R. Jackson, J. T. Williams, D. R. Wilton, S. B. Baumann, and A. C. Papanicolaou, "Computational aspects of finite element modeling in EEG source localization," IEEE Transactions on Biomedical Engineering, vol. 44, no. 8, pp. 736-752, 1997.

[54] H. Hallez et al., "Review on solving the forward problem in EEG source analysis," Journal of NeuroEngineering and Rehabilitation, vol. 4, no. 1, pp.1- 46, 2007.

[55] R. Grech et al. "Review on solving the inverse problem in EEG source analysis," (in eng), J Neuroeng Rehabil, vol. 5, pp. 1- 25, 2008.

[56] M. A. Jatoi, N. Kamel, A. S. Malik, and I. Faye, "EEG based brain source localization comparison of sLORETA and eLORETA," (in eng), Australas Phys Eng Sci Med, vol. 37, no. 4, pp. 713-21, 2014.

[57] E. Wan and A. Nelson, "Neural Dual Extended Kalman Filtering: Applications In Speech Enhancement And Monaural Blind Signal Separation," Neural Networks for Signal Processing - Proceedings of the IEEE Workshop, 2000.

[58] E. A. Wan and A. T. Nelson, "Dual Extended Kalman Filter Methods," in Kalman Filtering and Neural Networks, pp. 123-173, 2001.

THIS PAGE IS INTENTIONALLY LEFT BLANK.